

pected to increase with the compound nucleus excitation energy in the symmetric fission region around mass 118. Our data, although not conclusive, indeed show this trend. For strongly asymmetric mass splits ($\mu_H > 140$), where the total deformation of the scission configuration is not strongly influenced by introducing shell corrections in the potential energy surface, the kinetic energy is almost independent on the excitation energy. This shows also that the fission mode is not, or very weakly, coupled to the quasiparticle excitations.

As the (γ, f) and (γ, nf) cross sections for ^{235}U are not measured, the contribution of second chance fission in our experiments cannot be calculated directly. Based on the results of Caldwell *et al.*¹³ we found for the second chance fission contribution in our experiments⁷ on ^{238}U with 12-, 15-, and 20-MeV bremsstrahlung 0%, 15%, and 25%, respec-

tively. In view of the Γ_n/Γ_f values for ^{234}U , ^{235}U , ^{237}U , and ^{238}U , determined by Caldwell *et al.*,¹⁴ the second chance fission contribution is expected to be less in our ^{235}U photofission studies than in our experiments on ^{238}U . As discussed in our previous paper,⁷ the two effects of second chance fission, lowering the excitation energy and mass of the fissioning nucleus, are opposite and can possibly effect our results quantitatively. However, second chance fission is not expected to change the qualitative conclusions of this study.

This research was supported by the Nationaal Fonds voor Wetenschappelijk Onderzoek—Interuniversitair Instituut voor Kernwetenschappen. Thanks are expressed to the Linac team of our laboratory for the operation of the accelerator.

¹B. D. Wilkins, E. P. Steinberg, and R. R. Chasman Phys. Rev. C **14**, 1832 (1976).

²K. A. Petrzhak and G. A. Tutin, Yad. Fiz. **7**, 970 (1968) [Sov. J. Nucl. Phys. **7**, 584 (1968)].

³A. De Clercq, E. Jacobs, D. De Frenne, H. Thierens, P. D'hondt, and A. J. Deruytter, Phys. Rev. C **13**, 1536 (1976).

⁴W. Günther, K. Huber, U. Kneissl, H. Krieger, and H. J. Maier, Z. Phys. A **295**, 333 (1980).

⁵A. C. Shotter, J. M. Reid, J. M. Hendry, D. Branford, J. C. Mc George, and J. S. Barton, J. Phys. G **2**, 769 (1976).

⁶J. C. Mc George, A. C. Shotter, D. Branford, and J. M. Reid, Nucl. Phys. **A326**, 108 (1979).

⁷E. Jacobs, A. De Clercq, H. Thierens, D. De Frenne, P. D'hondt, P. De Gelder, and A. J. Deruytter, Phys. Rev. C **20**, 2249 (1979).

⁸H. W. Schmitt, W. M. Gibson, J. H. Neiler, J. F.

Walter, and T. D. Thomas, in *Proceedings of the First Symposium on the Physics and Chemistry of Fission, Salzburg, 1965* (IAEA, Vienna, 1965), Vol. I, p. 531.

⁹H. W. Schmitt, W. E. Kiker, and C. E. Williams, Phys. Rev. **137**, B837 (1965).

¹⁰L. I. Schiff, Phys. Rev. **83**, 252 (1951).

¹¹J. T. Caldwell, E. J. Dowdy, B. L. Berman, R. A. Alvarez, and P. Meyer, Phys. Rev. C **21**, 1215 (1980).

¹²E. Jacobs, H. Thierens, D. De Frenne, A. De Clercq, P. D'hondt, P. De Gelder, and A. J. Deruytter, Phys. Rev. C **21**, 237 (1980).

¹³J. T. Caldwell, E. J. Dowdy, R. A. Alvarez, B. L. Berman, and P. Meyer, Nucl. Sci. Eng. **73**, 153 (1980).

¹⁴J. T. Caldwell, E. J. Dowdy, B. Berman, R. Alvarez, and P. Meyer, Report No. LA-UR76-1615.

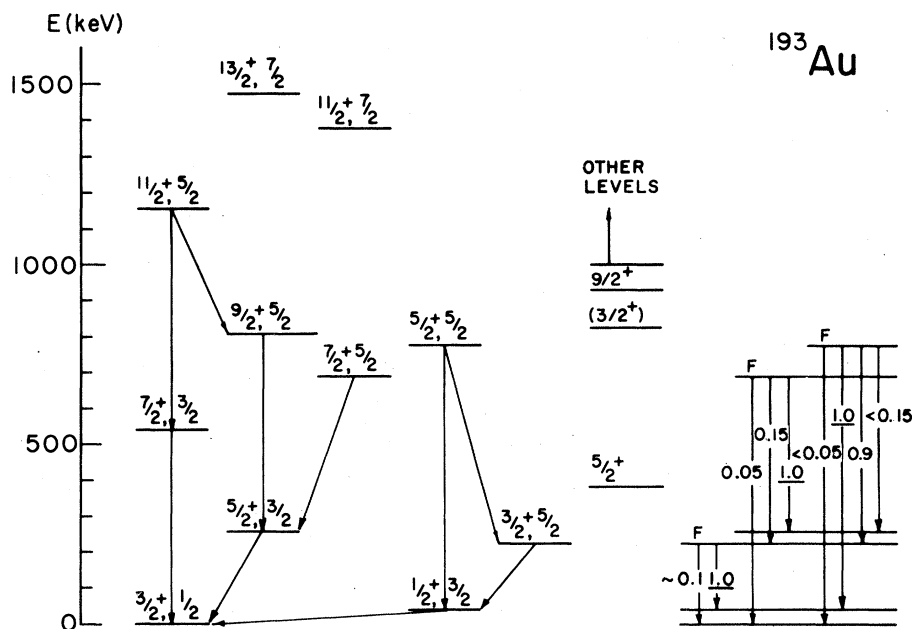


FIG. 1. The low-lying positive parity states in ^{193}Au . All known states up to 1 MeV are shown. States are labeled by the quantum numbers J^π, τ_1 . Arrows on the left show the strong $E2$ transitions observed between states with $\tau_1 = \frac{1}{2}, \frac{3}{2}, \frac{5}{2}$. On the right are shown the observed decay branches of $\tau_1 = \frac{5}{2}$ states that have τ_1 -forbidden $E2$ decay modes (marked by F). The relative reduced $E2$ transition intensities are shown. The $\frac{5}{2}^+$ state at 382 keV is believed to be mainly the $d_{5/2}$ configuration.

particular, the $E2$ branching ratio from the $\frac{3}{2}^+$ state should be regarded with some caution.) The $E2$ decay branches from the states $J^\pi, \tau_1 = \frac{7}{2}^+, \frac{5}{2}, \frac{5}{2}^+, \frac{5}{2}, \frac{3}{2}^+, \frac{5}{2}$ that are forbidden (marked by an F over the top of the transition arrow in Fig. 1) are clearly weak, supporting the proposition that the low-lying states of ^{193}Au can be described, to a good approximation, by the classification scheme of Ref. 1. It is worth noting that previous theoretical discussions of the same states in ^{193}Au in terms of the particle-vibrator⁸ and particle-asymmetric rotor model⁹ predicted the branching ratios for the decay of the $J^\pi, \tau_1 = \frac{3}{2}^+, \frac{5}{2}$ state to be 1.1:1.0 (Ref. 8) and 0.7:1.0 (Ref. 9). The most probable origin of the disagreement of these calculations with the data is that in the calculations of Refs. 8 and 9 the lowest $\frac{1}{2}^+$ state was given an $s_{1/2}$ character; whereas, as mentioned above, the ^{193}Hg decay scheme data,⁴ the similarity of the ^{193}Au and ^{195}Au excitation spectra, combined with the $^{194}\text{Pt}(^3\text{He}, d)^{195}\text{Au}$ data,¹¹ suggest that the $s_{1/2}$ strength lies above 1 MeV.

In conclusion, our experimental data indicate that ^{193}Au is, to a good approximation, describable

by the supersymmetric scheme of Ref. 1. However, in order to fully understand the extent to which this scheme can be applied in this region, further work is required. In particular, it is necessary to understand whether or not the set of nuclei ^{190}Os , ^{191}Ir , ^{192}Pt , ^{193}Au , and ^{194}Hg (with approximate $d_{3/2}$ subshell occupancies of 0, 1, 2, 3, and 4) all belong to the same supermultiplet. In addition, higher representations with $\sigma_1 < \sigma_{1, \text{max}}$ must be found and their decays studied, as in the case of the corresponding doubly-even nuclei.² In ^{193}Au a state at 828 keV is consistent with the assignment $J^\pi, \tau_1 = \frac{3}{2}^+, \frac{1}{2}$, and $\sigma_1 = \sigma_{1, \text{max}} - 1$. Finally, it should be noted that the example discussed here can also be related to a microscopic model proposed by Ginocchio.¹²

I wish to thank F. Iachello for the many discussions leading to this study, and J. Ginocchio for pointing out the relation between the above supersymmetry and his microscopic model. This work was supported in part by the U. S. Department of Energy, Contract No. DE-AS05-80ER10599.

menta have units MeV/c, and all parameters used here have units consistent with these choices. The form factors describing the axial current have been obtained in an earlier work.^{7,8} In the energy range which we are considering they are given by

$$|F_A|^2 = |\mathcal{F}_A|^2 f_A^2, \quad (5)$$

$$|\mathcal{F}_A|^2 = \frac{(3.61 \times 10^1 + 6.13 \times 10^{-1} q_0)}{[(q_0 - \alpha)^2 + \beta^2]}, \quad (6a)$$

$$f_A(q^2) = (1.0 - q^2/M_A^2)^{-2} M_A = 912 \text{ MeV}, \quad (6b)$$

$$F_A^{(3)} = \pm F_A / \sqrt{2}.$$

These form factors were obtained from pion photoproduction data and yield reasonable results for muon capture and for neutrino reactions in deuterium at LAMPF energies.^{7,8} There is no reason, however, to expect these form factors to accurately extrapolate to threshold neutrino processes. What we do here, therefore, is use the available neutral current neutrino results to modify the existing form factors in such a way that they reproduce this data and also do not change significantly the previous results for muon capture, neutrino reactions at LAMPF energies, pion capture, and pion photoproduction. This requirement fixes the choice for the form factors.

Because the measurement for the neutral current cross section is averaged over the reactor spectrum it is necessary to unfold the spectrum in order to obtain the elementary particle model¹³ form factors. The results obviously depend upon the spectrum chosen. We therefore use four spectra in current use, namely those by Avignone and Greenwood³ (AG), Davis *et al.*⁴ (DVMS), Borovoi⁵ *et al.* (BDK), and an experimental spectrum¹⁴ deduced from the reaction $\bar{\nu}_e + p \rightarrow n + e^+$. We then use the form factors so obtained along with the corresponding spectrum to calculate $\langle \sigma(\bar{\nu}_e d \rightarrow nne^+) \rangle$. What we are doing therefore, is checking whether the Reines, Sobel, and Pasierb (RSP) results for $\langle \sigma(\bar{\nu}_e d \rightarrow nne^+) \rangle$ are consistent with their results for $\langle \sigma(\bar{\nu}_e d \rightarrow np\bar{\nu}_e) \rangle$ and any of the spectra currently in use. We note that because the observed value for $\langle \sigma(\bar{\nu}_e d \rightarrow nne^+) \rangle$ is somewhat below the theoretical value used by RSP for the same cross section, this tends to increase our values for R slightly relative to their calculations. This is because our $(\sigma_{ncd})_{\text{exp}}/(\sigma_{ncd})_{\text{th}}$ is always unity, but a smaller neutral current cross section will in this model lead to smaller form factors and, hence, a smaller $(\sigma_{ccd})_{\text{th}}$. As a check we also used the AG

spectrum combined with their value³ for $\langle \sigma(\bar{\nu}_e d \rightarrow nne^+) \rangle$ as a check on this procedure.

We find that when we attempt to satisfy the criteria mentioned above, we can do so by varying the parameters α and β of Eq. (6), an appropriate approximation of the fit used in the earlier work mentioned. The original fitting of these was relatively insensitive to the data used to obtain them, but the threshold processes are very sensitive to them. We obtain our α and β by requiring that $\langle \sigma(\bar{\nu}_e d \rightarrow np\bar{\nu}_e) \rangle$ be fit in such a way that any induced variation in the pion photoproduction cross sections of the original fit be minimized. In all cases variations are less than 5% in all data, including the neutrino cross sections and muon capture rates obtained in our earlier paper. From the matrix elements^{7,8} $|M(\nu^2 H \rightarrow nne^+)|^2$ and $|M(\nu^2 H \rightarrow np\bar{\nu}_e)|^2$ obtained in our earlier work, setting F_V , the vector form factor to zero, we obtain values for the appropriate cross sections.

In Table I we list the values obtained for α , β , and $\langle \sigma(\bar{\nu}_e^2 H \rightarrow nne^+) \rangle$, and in Fig. 1 we plot the cross sections for $\bar{\nu}_e + {}^2\text{H} \rightarrow n + n + e^+$ for the above mentioned values of α and β for neutrino energy from threshold to 10 MeV. The errors in the procedure used here come primarily from errors expected in form factors induced by an error of roughly 20% in the measured $\langle \sigma(\bar{\nu}_e^2 H \rightarrow np\bar{\nu}_e) \rangle$ data. In addition, a rough estimate of the electromagnetic part of the final state interaction yields a potential error of up to 10%, yielding a total in the 25–30% range.

Using the R value defined by Reines *et al.*,¹ $R = [(\sigma_{ccd})_{\text{exp}}/(\sigma_{ccd})_{\text{th}}]/[(\sigma_{ncd})_{\text{exp}}/(\sigma_{ncd})_{\text{th}}]$ and recalling that because $(\sigma_{ncd})_{\text{exp}}$ was used to fit $(\sigma_{ncd})_{\text{th}}$, $(\sigma_{ncd})_{\text{exp}}/(\sigma_{ncd})_{\text{th}} = 1$ in our case, we obtain the values for R given in the second column of Table II. Finally, to examine the oscillation hypothesis we assume the experimentally determined spectrum is indeed an oscillated one and in turn as-

TABLE I. Spectrum averaged cross sections corresponding to the four spectra in general use are tabulated along with the corresponding values of α and β .

Spectra	α	β	$\langle \sigma(\bar{\nu}_e^2 H \rightarrow nne^+) \rangle \times 10^{-45} \text{ cm}^2$
AG	3.72	2.76	1.81
BDK	3.52	2.95	1.76
DVMS	3.75	2.47	1.51
Experimental	3.77	2.25	1.35